Modeling the Dynamic Hygrothermal Behavior of Biobased Construction Materials

Samuel DUBOIS*[1], Arnaud EVRARD[2], Frédéric LEBEAU[1]

[1]Dept. STE, Gembloux Agro-Bio Tech, University of Liege, Belgium

[2]Architecture et Climat, Université Catholique de Louvain, Belgium

*Corresponding author, supported by a F.R.I.A Grant,
Address: Dept. of environmental sciences and technologies, Gembloux Agro-Bio Tech, 2 Passage des déportés, 5030 Gembloux, Belgium (s.dubois@doct.ulg.ac.be)

KEYWORDS

Ham Modelling, Moisture Buffer Value, Lime Hemp Concrete, Hygroscopic, Latent Heat

STATUS

Published in*:

Journal of Building Physics, 2014

**Minor changes have been made compared to the original version*

ABSTRACT

The construction materials with high moisture exchange capacity may have a strong impact on indoor climate conditions as well as on energy performance of buildings. Crop-based materials, characterized by their high porosity and hygroscopic properties, belong to this category. Modeling their hygrothermal behavior with accuracy is thus particularly relevant for an efficient building design. A transient Building Element Heat Air and Moisture (BEHAM) model is developed in *COMSOL Multiphysics* to simulate the moisture exchange between a Lime-Hemp Concrete bloc and surrounding air during a Moisture Buffer Value (MBV) evaluation test.

The simulation results are compared to well-validated BEHAM software with the help of performance criteria. The proposed model shows a slightly better efficiency in the characterization of both moisture exchange and latent heat effect phenomena. In addition, it offers advantages in terms of flexibility and transparency as well as further evolution potential.

1. INTRODUCTION

Many authors (Padfield, 1999; Peuhkuri et al., 2005; Osanyintola and Simonson, 2006; Rode and Grau, 2008; Abadie and Mendonça, 2009, Li et al., 2012) have studied the capacity of porous hygroscopic materials to dampen the indoor humidity variations through moisture exchange, which is usually referred as the "Moisture buffer effect". The moisture exchange capacity is directly related to their porous structure as the latter will determine the sorption and capillary behavior as well as the transport coefficients. Crop-based insulation materials, which have recently appeared as a serious candidate in the search of sustainable and energy-efficient materials, have typically a strong buffer performance as both their moisture storage and transfer capabilities are high. The impact of such materials on the moisture balance at room or building level is thus typically non-negligible, like often stated for traditional materials. Moreover, ignoring their specific hygric behavior might lead to an incorrect prediction of direct and indirect energy demands for heating/cooling the building because of latent heat effects, comfort conditions modifications, and the dependence of heat transport parameters on moisture content (Osanyintola and Simonson, 2006; Tariku et al., 2010a). Is it thus important to solve with accuracy the transient and coupled balance equations that govern heat and moisture transport in those porous media.

Traditionally, models which deal with detailed Heat, Air and Moisture (HAM) analysis of envelope response have been focusing mainly on one envelope component at a time. For that reason they are called Building Element Heat, Air and Moisture (BEHAM) models. The origin of such tools is found in the Glaser's method (Glaser, 1959), a 1D calculation method for designing moisture-safe walls that is based on the description of steady-state diffusion. Later, in the 90's, the first physical models accounting for complex diphasic water transport in transient conditions were developed (Pedersen, 1991; Künzel, 1995; Häupl et al., 1997). They took profit of the knowledge acquired in the mathematical description of porous media since Philip and De Vries work (Philip and De Vries, 1957) as well as the progress in numerical resolution techniques and power. These models are always based on partial differential equations (PDEs) solved with finite elements or volumes methods on multilayered components of the envelope. Till today, many BEHAM computer software were developed and some commercialized (Hagentoft et al., 2004; Janssens et al., 2008). The description of the moisture flows is often classificatory. It can have several levels of complexity ranging from diffusivity models, where moisture content is used driving potential, to conductivity model with the actual thermodynamic driving potentials (Scheffler and Plagge, 2010). The most complex models incorporate pore space mathematical description which is used to obtain the hygrothermal transport and storage functions.

Lately, several authors (Kalagasidis, 2004; van Schijndel, 2009; Tariku et al., 2010a) have pointed out the possibility of using a single computational environment to combine different

building simulation tools. In this way, a whole building HAM model is more easily achievable, comprising indoor air and of envelope description tools as well as HVAC systems contributions. In the *Matlab/Simulink* popular environment, *COMSOL Multiphysics* (formerly *FemLab*) seems to be particularly interesting to manage the multidimensional PDE-based BEHAM problems (Tariku et al., 2010b; van Schijndel, 2009). It offers evident advantages in terms of modularity, transparency and ease of use. This answers the need for research-oriented modeling where lots of available tools are still opaque with little access to equations or material functions. In Tariku et al. (2010b) a *COMSOL* heat, air and moisture transfer model already passed successfully the standard *HAMSTAD* benchmarks exercises, proving its ability to solve complex transient problems.

The objective of this paper is to test the ability of a *COMSOL Multiphysics* model to simulate the coupled heat and moisture transfer taking place inside a crop-based material. For this purpose, a simple case study at material scale is used, dedicated to the characterization of hygroscopic products: the Moisture Buffer Value (MBV) test. This experimental protocol highlights the moisture exchange capacity of materials in the hygroscopic moisture content region. A material sample is continuously weighed and is subject to a normalized humidity cycle in isothermal conditions. Unlike previous works on MBV experiment modeling, not only the measured mass variation of the sample will be compared to the model output but also its exchange surface temperature which varies trough latent heat effects. In this way, we can validate the complex thermal aspects linked to moisture transfers that are incorporated in the model. All simulated results will be compared to the outputs of *WUFI Pro*, a validated BEHAM analysis software, with the help of objective efficiency criteria providing a clear outlook on model performance.

2. MATHEMATICAL MODEL

2.1 Macroscopic conservation equations

It is assumed that the porous medium $\Omega \subset R^3$ is a multiphase system consisting of the solid matrix, a liquid water phase and a gaseous phase, comprising dry air and water vapor. Two conservation PDEs are developed, one for moisture mass and one for heat, on an averaged representative elementary volume (REV) (Bear, 1988). The following additional hypothesis are taken for the mathematical description : (1) The material is non-deformable and isotropic; for a non isotropic material, standard transfer coefficients have to be replaced by tensors; (2) the fluid phases do not chemically react with the solid matrix; (3) The moisture content of the material as vapor θ_v is considered negligible compared to the correspondent term in liquid phase; (4) The dry air pressure is constant (no air advection) and the total gas pressure gradient are considered negligible; (5) no liquid to ice phase change is considered; (6) there is a local thermodynamic

equilibrium between the different phases; (7) There is no thermal effects due to friction or compression; (8) thermal diffusion (Soret effect) is neglected; (9) no hysteresis phenomena are accounted for.

Equation (1) shows the governing macroscopic equation for moisture flow through a porous medium given those hypotheses.

$$\rho_l \frac{\partial \theta_l}{\partial t} = -\nabla \cdot \left(\boldsymbol{j_c^{M_l}} + \boldsymbol{j_d^{M_v}}\right) + \sigma^{M_{v+l}} \quad (1)$$

With the different moisture flux densities being $\boldsymbol{j_c^{M_l}}$, the capillary transport of liquid water and $\vec{\boldsymbol{j}}_{\boldsymbol{d}}^{\boldsymbol{M_v}}$, the diffusion of vapor. Each of these moisture flux densities can be expressed as a function of a driving potential using constitutive mass transport relations. In an unsaturated porous building material, where gravity plays a negligible role in normal operating conditions, the liquid water is subjected to the suction of the medium through capillary forces. The capillary pressure in a pore p_c represents the difference between gas and liquid pressure around the meniscus:

$$p_c = p_g - p_l \quad (2)$$

Liquid transfers due to capillarity go from low capillary pressure (or high moisture content) to high capillary pressure (low moisture content). Replacing advection of liquid water and diffusion of vapor with Darcy's and Fick's law, respectively, the final expression of moisture balance is presented in **Equation 3**.

$$\rho_l \frac{\partial \theta_l}{\partial t} = -\nabla \cdot (K_l \cdot (\nabla p_c + \rho_l \cdot \vec{g}) - \delta_v \cdot \nabla p_v) + \sigma^{M_{v+l}} \quad (3)$$

Applying the law of conservation of internal energy, the enthalpy change in an averaged volume element is determined by the divergence of heat flux density by conduction, enthalpy transport due to transfer of fluid phases and the presence of heat sink or source. The balance equation does not take into account transfers by radiation and assumes that the local thermal equilibrium hypothesis is valid.

$$\frac{\partial(\rho h)}{\partial t} = -\nabla \cdot \left(\boldsymbol{j_{cond}^{Q}} + \boldsymbol{j_c^{M_l}} \cdot h_l + \boldsymbol{j_d^{M_v}} \cdot h_v\right) + \sigma^{Q} \quad (4)$$

The enthalpies in right-hand side of Equation (4) are related to the temperature through:

$$h_l = c_l \cdot (T - T_0) \quad (5)$$

$$h_v = c_v \cdot (T - T_{sat}) + L + c_l(T_{sat} - T_0) \quad (6)$$

Where L is the latent heat of phase change (J/kg) for pure water at T_{sat} =100°C and 1atm. The total specific enthalpy in the REV in left-hand side of **Equation 4** turns into:

$$\frac{\partial(\rho h)}{\partial t} = (c_0 \rho_0 + \rho_l \theta_l c_l) \cdot \frac{\partial T}{\partial t} \quad (7)$$

Rewriting the heat conservation equation considering all the constitutive assumptions yields the final mathematical formulation implemented in the model:

$$(c_0\rho_0 + \rho_l\theta_l c_l)\cdot\frac{\partial T}{\partial t} = -\nabla\cdot(-\lambda\nabla T + K_l(\nabla p_c + \rho_l\vec{g})h_l - \delta_v\nabla p_v h_v) + \sigma^Q \quad (8)$$

2.2 Additional relations

Equations 3 and **8** form the system to be solved. Two relationships have to be formulated between the different moisture field variables (i.e. the moisture content θ_l, the vapor pressure p_v and the capillary pressure p_c) in order to limit the number of unknowns. As the local thermodynamic equilibrium hypothesis is assumed valid around the meniscus in a pore, the Kelvin's equation relates the capillary pressure to the relative humidity (RH). Relative humidity is of course linked to the vapor pressure through the vapor saturation pressure, which is a function of temperature that can be approximated by different empirical relations. The sorption isotherm of the material, also called moisture storage curve (MSC), provides the second necessary relation, between the moisture content and relative humidity or capillary pressure. For the description of this material function, the most ordinary technique is to gather experimental data and to use fitting curves with adjustable parameters for a continuous description on the whole RH range. These parametric curves can be purely empirical or physically-based. The latter technique supposes to use a pore system description. Here, the pore structure of the material is described by the model of Häupl and Fechner (2003). The pore size distribution analytical function is formulated as a sum of N pore size compartments (the modes of the distribution), each centered on a main value of the pores radius R_i (m). The moisture storage process up to the filled radius r is obtained by the integration of the pore size distribution function following the bundle of capillary representation. Ultimately the moisture storage curve $\theta_l(\varphi)$ is given by:

$$\theta_l(\varphi) = \sum_i^N \theta_i \cdot \left(1 - \left(1 + \left(\frac{2\sigma}{\rho_w R_v T\cdot\ln(\varphi)\cdot R_i}\right)^2\right)^{1-n_i}\right) \quad (9)$$

Where θ_i (m^3/m^3) is the partial volume of the ith pore size compartment and n_i its shape factor describing its width. With Kelvin's equation and the MSC, it is possible to re-write the conservation equations system on a unique moisture field variable. This only requires simple mathematical re-formulations.

In addition to the moisture variables connections, the other material properties have to be properly defined. The thermal conductivity, thermal capacity, liquid conductivity and vapor permeability are in reality function of the two dependent variables giving typically non-linear PDEs. In some particular cases they could be considered as constant parameters but when large ranges of moisture content or temperature are met in the material, these simplifications could

lead to incorrect predictions. In consequence, depending on the case study, these functions have to be characterized properly. When needed, the liquid water conductivity dependency on water content can be derived from the porosity model.

3. CASE STUDY

Modeling the hygrothermal behavior of a bio-based material is considered here a case study to evaluate the performance and flexibility of the model solved with *COMSOL Multiphysics* in comparison to a validated model. The output of each model was compared to measurement gathered during a typical dynamic experiment dedicated to the characterization of hygroscopic material: the Moisture Buffer Value determination. This experimental protocol highlights the moisture exchange capacity of materials by massing of a sample subjected to a normalized humidity cycle in isothermal conditions. But unlike previous works on MBV modeling, not only the measured mass variation of the sample will be compared to the model output but also the temperature at the exchange surface, which varies through latent heat effects. In this way, we can validate the complex thermal aspects linked to moisture transfers that are incorporated in the model. The experimental validation will be conducted on a typical bio-based material: the Lime-Hemp Concrete (LHC).

3.1 MBV determination protocol

The need for a standardized parameter to characterize the moisture exchange capacity of materials led to the definition of MBV during the *NORDTEST* project (Peuhkuri et al., 2005) together with the proposal of a dynamic experimental protocol for materials classification. The practical MBV is defined as :*''the amount of water that is transported in or out of a material per open surface area, during a certain period of time, when it is subjected to variations in relative humidity of the surrounding air''* (Peuhkuri et al., 2005). Concretely, the samples are subject to cyclic step changes in relative humidity at a constant temperature of $23\,°C$ and are weighed regularly. The cycle is composed of a moisture uptake phase during 8 hours at 75% RH followed by moisture release during 16 hours at 33% RH (**Figure 1**) and is repeated until constant mass variation between 2 consecutive cycles is reached. This experimental value is a direct measurement of the amount of moisture transported to and from the material for the given exposure cycle.

Another approach might be used to predict the MBV of a material. Indeed, a theoretical value, called the ideal MBV, can be computed analytically using semi-infinite solid theory and Fourier series without transfer resistance at exchange surface (Peuhkuri et al., 2005). There is always a disagreement between measured and analytically calculated MBV due to the dynamic nature of the experimental protocol and film resistance on specimen exchange surface.

3.2 Lime-Hemp Concrete material

LHC are types of innovative concretes made out of the mix of hemp shivs (the woody core of industrial hemp stalk) and lime-based binders. With appropriate mixing proportions, they can be used in various applications like walls, roof insulation or even plasters (Evrard and De Herde, 2010). Many authors worked on LHC characterization and provided a set of physical and hygrothermal parameters for different mixes (Collet et al., 2008; Samri, 2008; Evrard and De Herde, 2010). The pore size distributions of the mixes or individual components were assessed by some of them with mercury porosimetry technique. There seems to be three general classes of pores: the microscopic porosity in the lime matrix (with peaks at ~0.05µm and ~0.5µm), the mesoscopic porosity in the hemp shivs (~10µm) and macroscopic porosity between de shivs in the binder (>1mm). **Figure 1a** shows a slice view of one hemp shiv obtained by X-ray microtomography. The high total porosity of the vegetal particle can be clearly seen with the typical tubular structure of the meso-scopic pores. **Figure 1b** shows a slice of a LHC sample, with mix proportions for wall casting, also obtained by tomography. The arrangement of the particles (appearing in grey due to low density) inside the binder (appearing in black due to high density) is visible with resulting macroporosity.

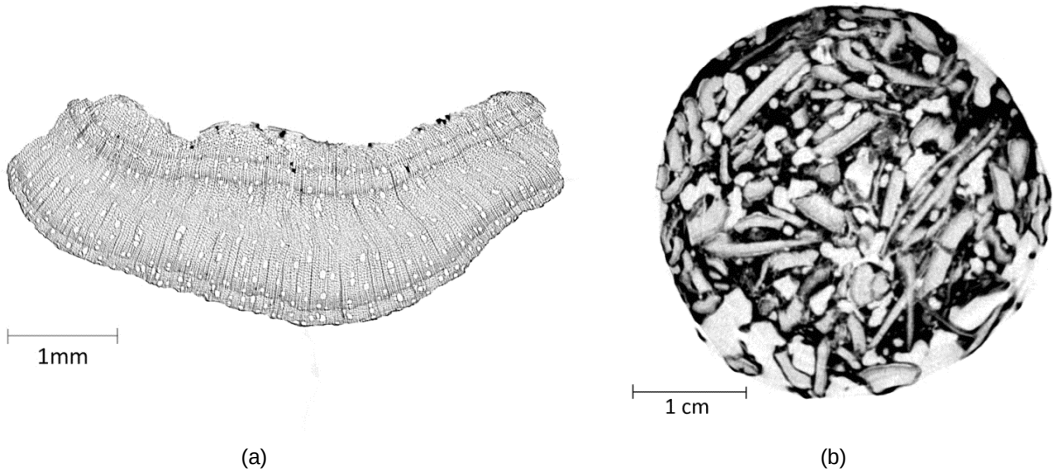

Fig. 1. Microtomography slices: a hemp shiv (a); a Lime-Hemp sample for wall casting application (b)

Table 1 compares the LHC material to some current construction materials with regard to different physical properties. Three main parameters are chosen as hygrothermal performance indicators: the thermal conductivity, the thermal effusivity and the ideal MBV. Thermal conductivity express the tendency of the material to allow heat to pass in steady-state conditions and lower values are thus favorable; thermal effusivity is an indicator of the heat exchange capacity of the material with its environment and high value are desirable to use thermal inertia effects; ideal MBV is an indicator of moisture buffering capacity of the material and high values are desirable to use natural damping of indoor humidity. This ideal MBV is here computed to

express the exchange capacity of the material on a 33/75%RH cycle and, as said before, it is derived from steady state parameters.

Table 1. LHC compared to standard construction materials.

	Density ρ	Total open porosity ε	Therm. conductivity λ	Therm. effusivity b	Ideal MBV 33-75
	kg/m^3	–	$W/(mK)$	$W \cdot s^{0.5}/(m^2K)$	$g/(m^2.\%RH)$
Spruce (parallel to grain)	455	0,73	0,23	396,2	6,694
Oak (parallel to grain)	685	0,72	0,3	555,2	5,565
Pumice concrete	664	0,67	0,14	281,1	5,307
Aerated Clay brick[c]	672	0,67	0,12	261,8	5,307
Straw bale[a]	100	0,9	0,085	130,4	5,247
Wood wool panel	450	0,55	0,08	232,4	4,424
Lime-hemp wall-mix[b]	440	0,73	0,115	281,0	3,783
Expanded clay concrete	700	0,67	0,13	278,1	3,086
Cellulose Insulation[c]	55	0,93	0,036	71,0	2,893
Aerated concrete (500kg/m³)	500	0,77	0,12	225,8	1,963
Extruded brick	1650	0,41	0,6	917,3	1,668
Oak (radial)	685	0,72	0,13	365,5	1,330
Sand-lime blocks	1900	0,29	1	1270,8	1,254
Spruce (radial)	455	0,73	0,09	247,8	1,217
Concrete W/C=.5	2300	0,18	1,6	1768,6	1,064
Manufactured brick	1725	0,38	0,6	937,9	0,402
Mineral wool	60	0,95	0,04	45,2	0,000
Extruded polystyrene (XPS)	40	0,95	0,03	42,4	0,000

Source : ***IBP Institute***
[a]Jakub Wihan, 2007
[b]Evrard and De Herde, 2010
[c]Masea Database

3.3 Test platform

A HPP749 (*Memmert*) climatic chamber was used to carry out the MBV humidity cycles in an isothermal closed environment. This device was upgraded with an additional dehumidification stage consisting of an AD 21-138 (*Aircraft*) refrigerating dryer in order to improve its performance. As the average air velocity in the chamber is necessary to determine the vapor diffusion resistance factor at the surface of the material, it was measured in the horizontal direction with an hot-wire anemometer 8465-300 (*TSI*). It showed an average value of $0.135 \pm 0.03\ m/s$.

The tested material is a LHC wall-mix (Evrard and De Herde, 2010) from the same origin as samples used by Evrard (2008). The binder is the widespread Tradical PF70 mixed with *Chanvribat* hemp particles. The components mix proportions of the bloc are given in **Table 2**.

The LHC sample bloc has a unique moisture exchange surface of 150x150mm and a thickness of 75mm, which is stated sufficient given the theoretical moisture penetration depth during the MBV experiment. Lateral and back faces are isolated from water exchange with polyethylene film and tape (**Fig. 2**). One SHT75 (*Sensirion*) sensor is implemented 15cm above the sample in

order to monitor the evolution of humidity and temperature in the chamber. Finally, a DS18B20 (*Dallas*) temperature sensor is placed on the surface of the material with a small thermal insulation cap on top of it. This sensor is dedicated to the detection of the latent heat effect. The insulation cap was stated necessary to monitor the actual surface temperature, avoiding the influence of the surrounding air. Once instrumented, the sample was placed inside the chamber on an M-Power (*Sartorius*) laboratory scale with a 0-3100g range and 0.01g resolution. This scale was monitored every 5 minutes trough its RS232 output via a *LabVIEW* acquisition program. The whole experimental set-up is shown on **Figure 3**.

Table 2. Composition of the sample bloc

LHC wall mix	(%mass)	kg if 20kg of Chanvribat
Chanvribat	17	20
Tradical PF70	33	40
Water	50	60
Total	100	120

Fig. 2. LHC bloc with sealed lateral faces

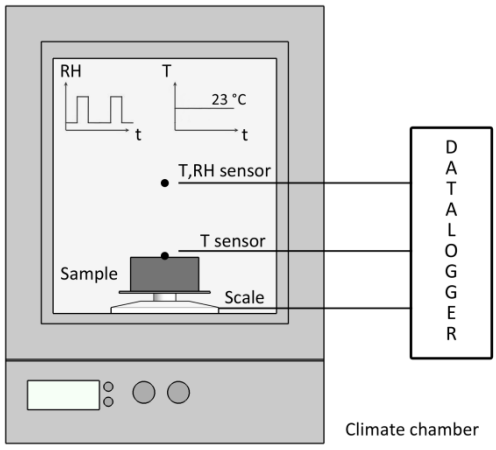

Fig. 3. Experimental set-up

4. MODELING PROCEDURE

4.1 Equations re-formulation

The incorporation of the mathematical model in *COMSOL Multiphysics* offers the advantage of flexibility in the mathematical formulation. Indeed, the user can choose the equations set complexity as well as the mathematical expressions for the moisture retention curve and other material functions. During the MBV solicitation cycle, which lies in the range 33/75%RH, the LHC bloc will be mainly subject to hygroscopic storage and vapor water transport. In consequence, the conservation equations should be simplified in order to minimize the computational time. Even if the MBV determination experiment is conducted in isothermal conditions, the heat balance equation is still necessary to account for latent heat effects in the material. Again, the model used in this paper offers the advantage of being fully modular.

The chosen dependant variables for simulations are temperature and relative humidity. In addition, no liquid water transport is accounted for, enthalpy transport is accounted for, and no source/sink term is necessary. The PDEs will be solved in 1 dimension giving the following final expressions for moisture and heat conservation equations:

$$\xi \cdot \rho_l \cdot \frac{\partial \varphi}{\partial t} = \delta_{v0} \cdot \frac{\partial^2(\varphi \cdot p_{sat}(T))}{\partial x^2} \tag{10}$$

$$(c_0\rho_0 + \rho_l\theta_l c_l)\frac{\partial T}{\partial t} = \frac{\partial}{\partial x}\left(\lambda_0 \frac{\partial T}{\partial x} + \delta_{v0} \cdot \frac{\partial(\varphi \cdot p_{sat}(T))}{\partial x} \cdot h_v\right) \tag{11}$$

Water is consider as pure water with liquid density $\rho_l = 1000\ kg/m^3$, liquid specific heat capacity $c_l = 4187\ J/(kg \cdot K)$, vapor specific heat capacity $c_v = 2000\ J/(kg \cdot K)$ and latent heat of vaporization $L = 2257\ kJ/kg$. The following material parameters are considered constant with values for the material in dry state, taken from previous measurements (Evrard, 2008): $\rho_0 = 440\ kg/m^3$, $\lambda_0 = 0.115\ W/m$, $c_0 = 1560\ J/(kg \cdot K)$ and $\delta_{v0} = 4.12E-11\ kg/(m \cdot s \cdot Pa)$.

4.2 Moisture retention curve calibration

The moisture capacity ξ was obtained by calibrating the Häupl & Fechner's porosity model with experimental data for LHC. Indeed, the multimodal moisture storage function was fitted on experimental points that were previously obtained by Evrard and De Herde (2010) with pressure plate and salt solutions methods. Literature data from mercury intrusion porosimetry on LHC helped to select the main pore radii $R2$ and $R3$ in accordance with the real pore size distribution. The main pore radius $R1$ has no physical meaning and is used as an artificial mean to account for surface adsorption, which can be considered similar to capillary condensation in very small

pores. The selected parameters are given in **Table 3** and the obtained porosity distribution is shown on **Figure 4**. This calibration of the pore space function in the BEHAM model opens large perspectives for further work on LHC that should address their behavior in the overhygroscopic moisture content region.

Table 3. Moisture storage function parameters

Main radius			Partial volume			Shape parameter		
R1	R2	R3	θ_1	θ_2	θ_3	n_1	n_2	n_3
5.6E-4µm	0.08µm	0.5µm	0.11	0.133	0.33	1.09	1.32	1.20

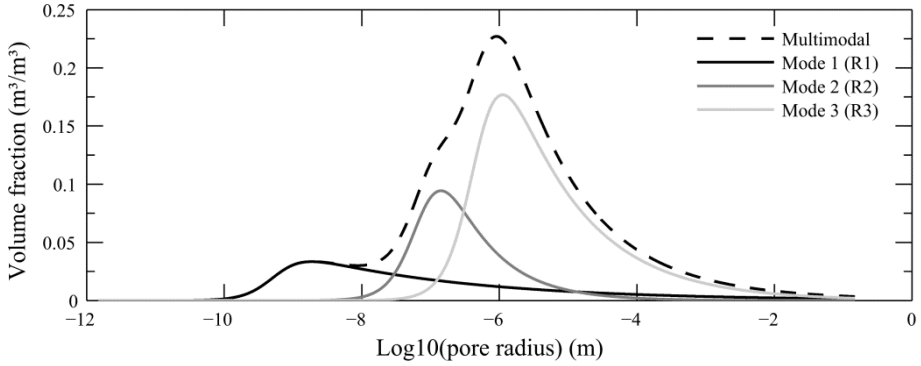

Fig. 4. The LHC multimodal pore size distribution function with highlighting of the different pore space compartments

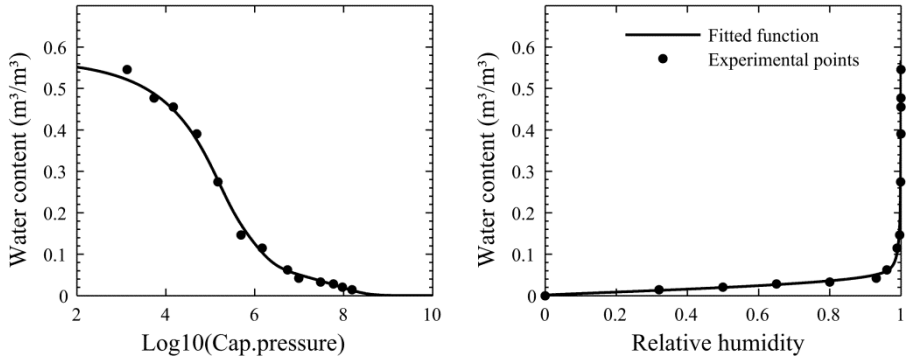

Fig. 5. Fitted moisture content of LHC as a function a capillary pressure and relative humidity

4.3 Boundary and initial conditions

Referring to **Figure 6**, we can write the following boundary and initial conditions for moisture transport:

$$\left(\boldsymbol{j}^{\boldsymbol{M_v}}\right)\cdot\boldsymbol{x} = \frac{\left(\varphi_\infty p_{sat,\infty} - \varphi_s p_{sat,s}\right)}{Z_s} \qquad x = 0 \qquad (12)$$

$$\frac{\partial \varphi}{\partial x} = 0 \qquad x = L \qquad (13)$$

$$\varphi(x,0) = \varphi_0 \qquad 0 < x < L \qquad (14)$$

where $\boldsymbol{j^{M_v}}$ is the moisture flux density $(kg/m^2\,s)$, φ_∞ / $p_{sat,\infty}$ the relative humidity / saturation pressure in the climatic chamber, and φ_s / $p_{sat,s}$ the relative humidity / saturation pressure at the exchange surface.

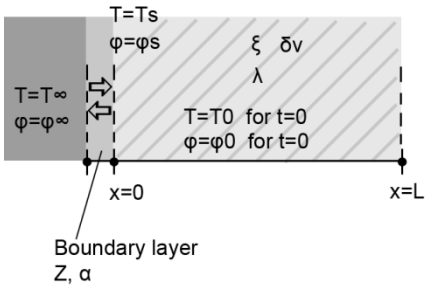

Fig. 6. Domain and boundary conditions

The vapor diffusion resistance factor Z_s $(Pa/(kg \cdot m^2 \cdot s))$ characterizes the moisture transfer resistance that exists on the material surface and slows down the moisture exchange. Its value is fixed to $5 \cdot E7\ Pa/(kg \cdot m^2 \cdot s)$ which is the usually accepted value for environments with an ambient air velocity around $0.1\ m/s$ (Peuhkuri et al., 2005). It's similar to a value of $Z_{s,v} = 360\ s/m$ when the surface flux density is written in terms of absolute humidity:

$$\left(\boldsymbol{j^{M_v}}\right) \cdot \boldsymbol{x} = \frac{(v_\infty - v_s)}{Z_{s,v}} \qquad (15)$$

To calculate the accumulated moisture, Equation (16) is used.

$$G_v = \int_0^t g_v dt \qquad (16)$$

The resulting relative mass of the sample is given by:

$$m(t) - m_0 = G_v(t) * A \qquad (17)$$

where $m(t)$ is the mass of the sample at time t (kg), m_0 is the initial mass of the sample (kg) and A is the exchange surface area of the sample (m^2).

For heat transport, the boundary and initial conditions are given by:

$$\left(\boldsymbol{j^Q}\right) \cdot \boldsymbol{x} = \alpha \cdot (T_\infty - T_s) + \left[\left(\varphi_\infty p_{sat,\infty} - \varphi_s p_{sat,s}\right)/Z_s\right] \cdot h_v \qquad x = 0 \qquad (18)$$

$$\left(\boldsymbol{j^Q}\right) \cdot \boldsymbol{x} = \alpha \cdot (T_\infty - T_L) \qquad x = L \qquad (19)$$

$$T(x,0) = T_0 \qquad 0 < x < L \qquad (20)$$

with $\boldsymbol{j^Q}$ the heat flux density (W/m^2), T_∞ the chamber temperature $(°C)$, T_s the temperature at exchange surface $(°C)$ and T_L the temperature at the bottom of the sample $(°C)$. The convective

heat transfer coefficient α (W/m^2K) is fixed to $1{,}44E8/Z_{surf}$ according to (Peuhkuri et al., 2005).

The input data T_∞ and φ_∞ for ambient air variations used as boundary solicitation in the model are the measured RH and temperature from the experimental cycles, which might be quite different from the ideal step cycle. The initial conditions inside the bloc are fixed to $\varphi_0 = 55\%RH$ and $T_0 = 23.1°C$ to match real equilibrium conditions before the start of the test.

4.4 Numerical resolution

The two PDEs need to be solved simultaneously in order to obtain the desired temperature and humidity fields across the domain as well as the resulting heat and mass fluxes. *COMSOL Multiphysics* is based on finite-element resolution technique and provides an equation-based modeling module that allows users to encode their own PDEs equations. The latter is referred as "PDE interfaces module" (Tariku et al., 2010b). The two conservation equations were thus encoded in the following general form:

$$a\frac{\partial X}{\partial t} + \nabla \cdot \Gamma = 0 \tag{21}$$

where a is referred as the damping coefficient, X is the dependent variable and Γ is the conservative flux. In order to treat the MBV transient problem, the built-in time dependent explicit solver was used to get the variables fields. The time discretization consists of a free variable time stepping with a maximum time step fixed to 5 minutes, which corresponds to the boundary conditions variation step. Spatially, the domain is meshed with respect to the expected dependent variables gradients. The finite elements distribution density is increased near the exchange surface using a geometric progression.

The outputs of the *COMSOL* model are compared to results from the validated *WUFI Pro* BEHAM software. The simulation in *WUFI* was performed with the same material parameters and a piecewise moisture retention curve. However, boundary conditions were defined on an hourly basis and only the convective heat transfer coefficient can be encoded in the software.

4.5 Efficiency criteria and error indices

Three criteria were used to formulate an objective assessment of the models performance relatively to the MBV test simulations: the Nash-Sutcliffe efficiency coefficient (NSE), the percent bias (PBIAS) and the root mean square error (RMSE). Such indicators also provide a mean of comparison between the *COMSOL* model and the *WUFI Pro* software. The NSE is defined as one minus the sum of squared differences between simulated and observed values normalized by the variance of observed data:

$$NSE = 1 - \frac{\sum_{i=1}^{n}(X_{model,i} - X_{obs,i})^2}{\sum_{i=1}^{n}(X_{obs,i} - \bar{X}_{obs})^2} \quad (22)$$

where $X_{model,i}$ is the model predicted value for time step i, $X_{obs,i}$ is the experimental observation for the same time step and $\bar{X}_{obs}$ is the mean of all experimental values. A NSE coefficient of 1 means a perfect fit of the model to experimental data. If the indicator falls below zero that would imply that the residual variance is larger than data variance and thereby the mean value of observed data would be a better predictor that the model. The NSE also characterizes how well $(X_{obs,i}, X_{model,i})$ points fit the 1:1 line (identity line). The second indicator, the PBIAS, is defined as:

$$PBIAS = \frac{\sum_{i=1}^{n}(X_{obs,i} - X_{model,i})}{\sum_{i=1}^{n} X_{obs,i}} \cdot 100 \quad (23)$$

It indicates the average tendency of modeled data to systematically under or over-estimate the observed data. Finally, the RMSE is the most commonly used error index and is scale-dependent. A RMSE value of zero indicates a perfect fit to observed data.

Simulations can be judge satisfactory if the indicators stays in a predefined range. These acceptance values can be fixed to NSE > 0.8 and $|PBIAS| < 15\%$ in light of watershed modeling techniques, where accuracy issues were widely discussed (Moriasi et al., 2007). As RMSE is not normalized, it's more difficult to give a clear acceptance range.

5. RESULTS

5.1 Experimental results

Figure 7 shows the MBV humidity cycles and the mass variation of the sample measured experimentally. Numbers were assigned to four of the 24h cycles to facilitate the subsequent analyzes. For each cycle, the climatic chamber is capable of reaching a 33-70% RH transition in 20 minutes and 75-50% RH in 30 minutes. However, the ends of the two transitions are really slow and need further improvement to get closer to a step solicitation. The actual humidity values are also higher than expected, with an average of 40% during the low humidity phase (6.20PM-10.20AM) and 75.3% during the high humidity phase (10.20AM-6.20PM). This is partly due to poor calibration of the humidity sensors regulating the chamber. It is then necessary to take into account these conditions during the computer simulations and MBV determination.

The absorption/desorption dynamics can be seen trough the mass variation of the sample. The test starts with a desorption phase from initial equilibrium humidity, which is close to $55\%\ RH$ with an average of $55{,}1\%$ on the hour preceding the start of the test. As expected, the practical buffer value for LHC is lower than the ideal value (**Table 1**), with an average of

2.34 $g/(m^2 \cdot \%RH)$ on the four last cycles. This can be explained by surface resistance effect (boundary layer). **Figure 8** shows measurements details for the cycle number 1, chosen as reference cycle to illustrate LHC behavior. The latent heat effects resulting of the moisture movements can be clearly seen trough the surface temperature monitoring. The surface temperature remains above air temperature during absorption phase, with a mean value of $+0.30°C$ and a maximum of $+0.67°C$, and below air temperature during desorption, with a mean of $-0.07°C$ and a maximum of $-0.21°C$. The amplitude between the minimum and maximum surface temperature is $0.81°C$.

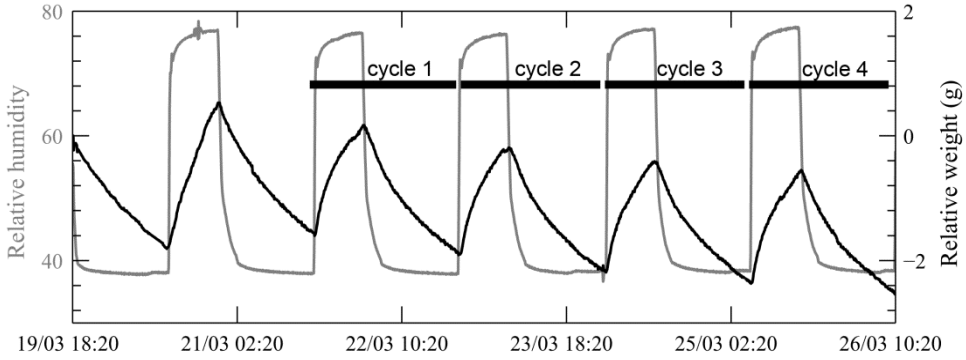

Fig. 7. The *MBV* protocol experimental curves and cycles numbers[2]

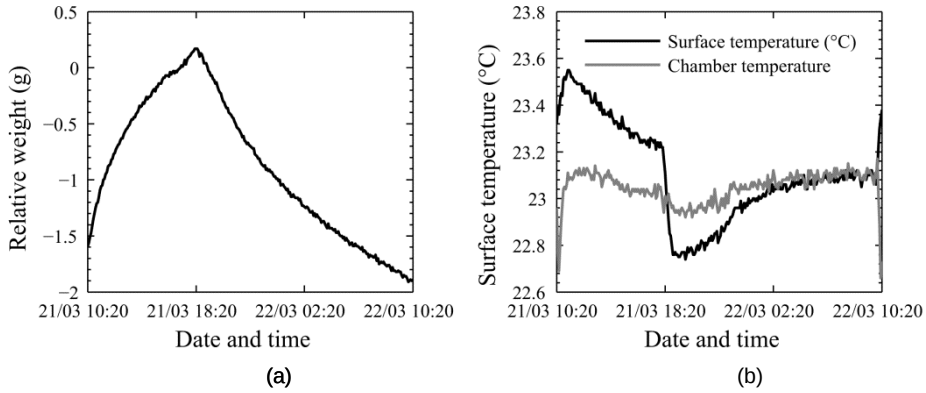

Fig. 8. Cycle number 1: relative mass variation of the sample (a); air temperature in the chamber and temperature at the surface of the bloc (b)

5.2 Mass variation modeling

Figure 9 presents the sample mass variation predicted by *COMSOL Multiphysics* and *WUFI Pro* models compared to measured data. Relative mass is defined in **Equation 17**. In addition, **Table 4** shows results expressed in terms of practical MBV for the four complete cycles with a value for absorption phase, another for desorption phase and the mean of these two phases. Both models provide similar results with a small over-evaluation of moisture exchange, larger in the case of *WUFI Pro* simulation.

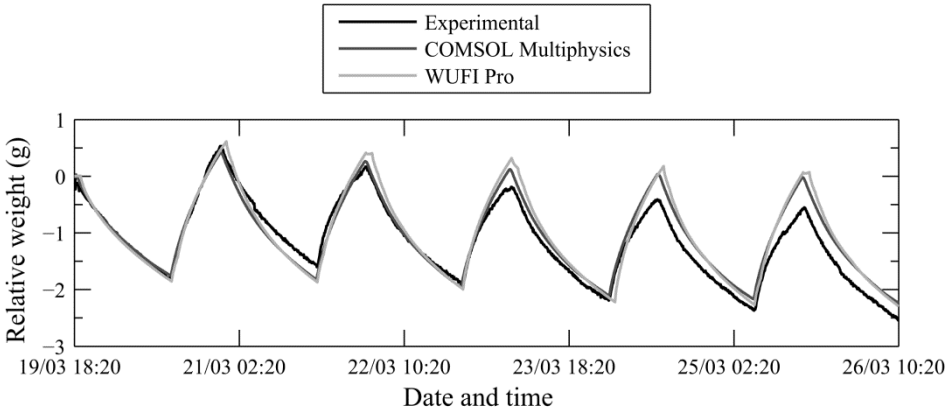

Fig. 9. Relative mass variation of the sample during the MBV determination cycles compared to models outputs

Table 4. $MBV_{practical}$ $(g/(m^2 \cdot \%RH))$ results for the experimental and the simulated data sets

	ΔRH	Cycle 1			Cycle 2			Cycle 3			Cycle 4		
		Abs.	Des.	Mean	Abs.	Des.	Mean	Abs.	Des.	Mean	Abs.	Des.	Mean
Experimental	~35.3%	2.13	2.57	2.35	2.15	2.52	2.34	2.24	2.44	2.34	2.27	2.51	2.39
COMSOL Multiphysics	~35.3%	2.41	2.73	2.57	2.61	2.81	2.71	2.70	2.74	2.72	2.67	2.78	2.72
WUFI PRO	~35.3%	2.67	2.91	2.79	2.91	3.16	3.04	2.88	3.03	2.96	2.94	2.98	2.96

The performance indicators were computed for the two models and are provided in **Table 5**. They give similar values for both modeling environments with a slightly better performance of the proposed model. Nash-Sutcliffe efficiency is above 0.8 in both cases, implying a satisfactory modeling. However, the PBIAS indicates clearly the overestimation tendency of the models, which stays below the 15% limit. Comparison between the PBIAS and RMSE points out a better performance of *COMSOL* simulation. To complete the analysis, correlation plots are represented in **Figure 10** showing scattering of $(X_{obs,i}, X_{model,i})$ points around the identity line. The dashed line represents the best linear regression between modeled and experimental points. A perfect model would of course give a regression line equal to identity line.

Table 5. Efficiency criteria for mass variation modeling

	NSE	PBIAS	RMSE
COMSOL Multiphysics	0.89	-7.51%	0.22g
WUFI PRO	0.84	-9.47%	0.27g

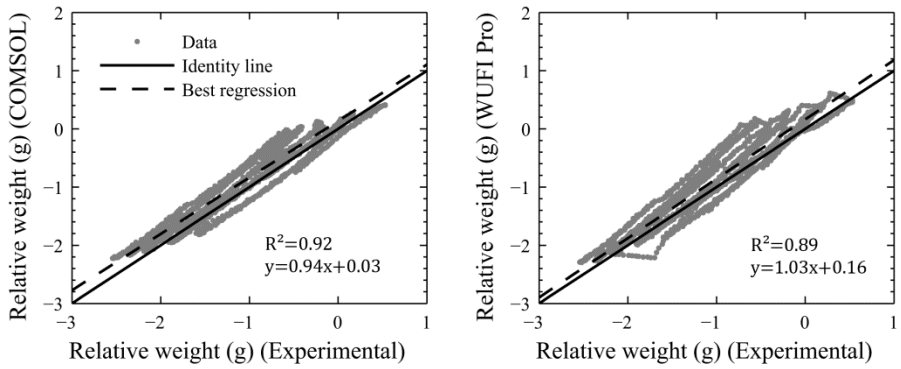

Fig. 10. Correlation plots of relative mass variation modeling

5.3 Surface temperature modeling

Surface temperature results are presented in **Figure 11**. The general shape of the temperature variation seems to be accurately predicted by both models in spite of a clear discrepancy for the amplitude. Temperature is systematically higher than observed during absorption phases and lower during desorption phases for both models. In other words there is an overestimation of surface latent heat effects.

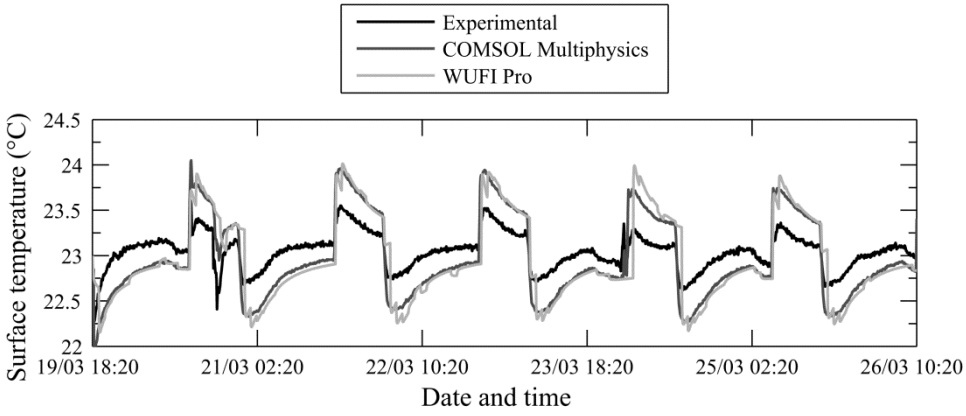

Fig. 11. Surface temperature of the sample during the MBV determination cycles compared to models outputs

Given the performance indicators, which are presented in **Table 6**, it is possible to evaluate quantitatively the accuracy of surface temperature description. The NSE is lower than zero for both models indicating very poor prediction. The PBIAS are really low due to the mathematical nature of this indicator, which only evaluate systematic over or under-prediction.

Table 6. Efficiency criteria for surface temperature modeling

	NSE	PBIAS	RMSE
COMSOL Multiphysics	-1.24	0.36%	0.295°C
WUFI PRO	-2.09	0.38%	0.346°C

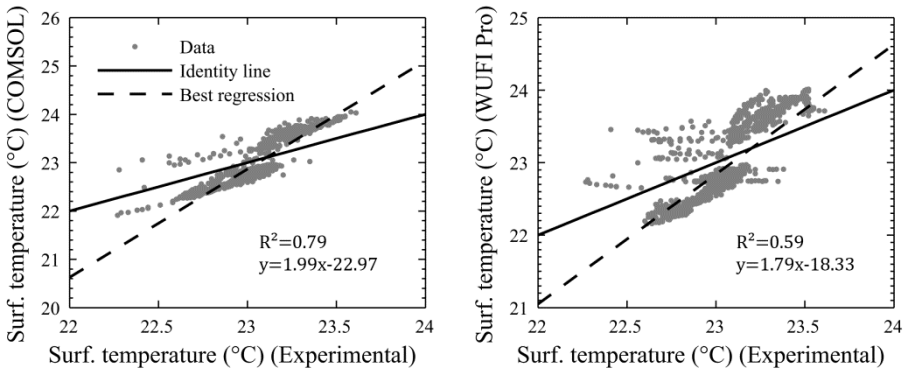

Fig. 12. Correlation plots of surface temperature modeling

The difference between the experimental and simulated data sets could be explained either by experimental bias or improper surface transfer coefficients definition. Anyway it was proved the *COMSOL* BEHAM model performs as well as the validated code. The surface temperature variation is really interesting to observe and its shape is correctly accounted for, translating a good characterization of involved phenomena. One of the remaining challenges is to evaluate correctly the impact of such effects on the thermal efficiency of materials that could bring some additional credit to the crop-based products.

6. CONCLUSIONS AND PERSPECTIVES

Accurate BEHAM models are necessary to account for moisture exchange capacity of hygroscopic materials, which can greatly influence the characterization of building performance. Lately, *COMSOL Multiphysics* was partially benchmarked and presented as a valuable alternative to standard BEHAM tools. It offers advantages in the research field, particularly with regards to its modularity and interoperability. In this paper, a MBV determination experiment was led to gather experimental data that could be compared to the output of a hygrothermal model developed in *COMSOL* computational environment. For this purpose, a complete MBV test platform was developed and improved with a surface temperature monitoring system. The studied material, the Lime-Hemp Concrete, belongs to crop-based materials, which are being widely promoted and have a strong moisture buffer capacity linked to their high porosity and hygroscopicity.

First, the partial differentials equations for heat and moisture transport were presented with associated relations and material functions. The model was then reformulated for the case study and calibrated for LHC characterization. In order to obtain an objective assessment of model performance, an efficiency indicator and two error indices were used as prescribed in watershed modeling field. Output data sets were compared to a validated BEHAM tool showing good agreement between the two software. As a conclusion, the *COMSOL* BEHAM tool is able to solve high MBV material behavior in an adaptable way. On the one hand, moisture exchanges

were predicted accurately by both models, i.e. the computed indicators remain within the limits sets with a slight advantage for *COMSOL*. On the other hand, resulting temperature variations on the surface of the specimen indicate an overestimation of latent heat effect amplitude for both computations. This marks the necessity of further research on crop-based products as well as additional parameters optimization. In this perspective, large opportunities are introduced by using such an HAM tool. It offers the possibility of solving problems in 1D, 2D or 3D with research oriented modularity. The incorporated description of porous space based on Häupl & Fechner (2003) gives the storage and transport function on the whole moisture content, which is promising in solving more complex building physics problems involving crop-based products. Finally, the interoperability of *COMSOL* allows for inverse modeling to optimize material parameters, taking advantage of software package like *DREAM* (ter Braak, 2006) in Matlab.

NOMENCLATURE

$\boldsymbol{c_0}$	(J/kgK)	Specific heat of the dry material
$\boldsymbol{c_\alpha}$	(J/kgK)	Specific heat of the α-phase
$\boldsymbol{h}$	(J/kg)	Total specific enthalpy stored in the porous material
$\boldsymbol{h_\alpha}$	(J/kg)	Specific enthalpy of the α-phase
$\vec{\boldsymbol{j}}_{\boldsymbol{c}}^{\boldsymbol{M_l}}$	$(kg/(m^2 s))$	Mass flux density of liquid water through capillary transport
$\vec{\boldsymbol{j}}_{\boldsymbol{d}}^{\boldsymbol{M_v}}$	$(kg/(m^2 s))$	Mass flux density of vapor through diffusion
$\vec{\boldsymbol{j}}_{\boldsymbol{cond}}^{\boldsymbol{Q}}$	(W/m^2)	Thermal conduction flux density
$\boldsymbol{K_l}$	(s)	Liquid water conductivity of the porous material
$\boldsymbol{p_c}$	(Pa)	Capillary pressure
$\boldsymbol{p_{sat}}$	(Pa)	Saturation vapor pressure
$\boldsymbol{p_\alpha}$	(Pa)	Pressure of the α-phase
$\boldsymbol{T}$	(K)	Temperature
$\boldsymbol{v}$	(kg/m^3)	Absolute humidity
$\boldsymbol{\delta_{v0}}$	$(kg/Pa\,.m.s)$	Vapor permeability of the dry porous material
$\boldsymbol{\delta_v}$	$(kg/Pa\,.m.s)$	Vapor permeability of the porous material
$\boldsymbol{\varepsilon}$	$(-)$	Total open porosity of the porous material
$\boldsymbol{\theta_\alpha}$	(m^3/m^3)	Volumetric fraction of the α-phase
$\boldsymbol{\lambda_0}$	(W/mK)	Thermal conductivity of the porous material in dry state
$\boldsymbol{\lambda}$	(W/mK)	Thermal conductivity of the porous material
$\boldsymbol{\xi}$	$(m^3/(m^3 \cdot \%RH))$	Moisture capacity
$\boldsymbol{\rho}$	(kg/m^3)	Total density of the material
$\boldsymbol{\rho_0}$	(kg/m^3)	Mass density of the dry porous material
$\boldsymbol{\rho_\alpha}$	(kg/m^3)	Mass density of the α-phase
$\boldsymbol{\sigma^{M_\alpha}}$	$(kg/(m^3 s))$	Mass source/sink terms for the α-phase
$\boldsymbol{\sigma^{Q}}$	(W/m^3)	Heat source/sink
$\boldsymbol{\varphi}$	$(-)$	Relative humidity

Subscripts

l	Related to liquid water
v	Related to water vapor
g	Related to the gaseous mixture of dry air and water vapor
a	Related to dry air

REFERENCES

Abadie, M. O. and Mendonça, K. C. (2009). Moisture performance of building materials: From material characterization to building simulation using the Moisture Buffer Value concept. *Building and Environment, 44*(2), 388-401.

Bear, J. (1988). Dynamics of fluids in porous media. Dover Publications, New York. 784 p.

Collet, F., Bart, M., Serres, L. and Miriel, J. (2008). Porous Structure and Vapour Sorption of Hemp-based Materials. *Constr. Build. Mater.*, 22, 1271–1280.

Evrard, A. and De Herde, A. (2010). Hygrothermal Performance of Lime-Hemp Wall Assemblies. *Journal of Building Physics, 34*(1), 5-25.

Glaser, H. (1959). Graphisches Verfahren zur Untersuchung von Diffusionsvorglinge*. Kalfetechnik, 10, 345-349.*

Hagentoft, C.-E., Kalagasidis, A. S., Adl-Zarrabi, B., Roels, S., Carmeliet, J., Hens, H. and Djebbar, R. (2004). Assessment Method of Numerical Prediction Models for Combined Heat, Air and Moisture Transfer in Building Components: Benchmarks for One-dimensional Cases. *Journal of Thermal Envelope and Building Science, 27*(4), 327-352.

Häupl, P. and Fechner, H. (2003). Hygric Material Properties of Porous Building Materials. *Journal of Thermal Envelope and Building Science, 26*(3), 259-284.

Häupl, P., Grunewald, J., Fechner, H. and Stopp, H. (1997). Coupled heat air and moisture transfer in building structures. *International Journal of Heat and Mass Transfer, 40*(7), 1633-1642.

Janssens, A., Woloszyn, M., Rode, C., Kalagasidis, A. S. and De Paepe, M. (2008). From EMPD to CFD : overview of different approaches for Heat Air and Moisture modeling in IEA Annex 41. Proceedings of the IEA ECBCS Annex 41 Closing Seminar, Conference, Denmark.

Kalagasidis, A. S. (2004). HAM-Tools : an integrated simulation tool for heat, air and moisture transfer analyses in building physics. Ph.D. Thesis, Dept. of Building Technology, Building Physics Division, Chalmers University of Technology, Sweden.

Kalagasidis, A. S., Weitzmann, P., Nielsen, T. R., Peuhkuri, R., Hagentoft, C.-E. and Rode, C. (2007). The International Building Physics Toolbox in Simulink. *Energy and Buildings, 39*(6), 665-674.

Künzel, H. M. (1995). Simultaneous heat and moisture transport in building components : one- and two- dimensional calculation using simple parameters. IRB Verlag.

Li, Y., Fazio, P. and Rao, J. (2012). An investigation of moisture buffering performance of wood paneling at room level and its buffering effect on a test room. *Building and Environment, 47*(1), 205-216.

Moriasi, D. N., Arnold, J. G., Van Liew, M. W., Bingner, R. L., Harmel, R. D. and Veith, T. L. (2007). Model evaluation guidelines for systematic quantification of accuracy in watershed simulations. *Transactions of the ASABE, 50*(3), 885-900.

Osanyintola, O. F. and Simonson, C. J. (2006). Moisture buffering capacity of hygroscopic building materials: Experimental facilities and energy impact. *Energy and Buildings, 38*(10), 1270-1282.

Padfield, T. (1999). The role of absorbent building materials in moderating changes of relative humidity. Ph.D. Thesis, Dept. of Structural Engineering and Materials, Technical University of Denmark, Denmark.

Pedersen, C. R. (1991). A transient model for analyzing the hygrothermal behavior of building constructions. Proceedings of the 3rd IBPSA, Conference, France.

Peuhkuri, R. H., Mortensen, L. H., Hansen, K. K., Time, B., Gustavsen, A., Ojanen, T. and Harderup, L.-E. (2005). Moisture Buffering of Building Materials. In C. Rode (Ed.): Department of Civil Engineering, Technical University of Denmark.

Philip, J. R., De Vries, D. A. (1957). Moisture movement in porous materials under temperature gradients. *Trans. Am. Geophys. Union, 38, 222-232*

Rode, C. and Grau, K. (2008). Moisture Buffering and its Consequence in Whole Building Hygrothermal Modeling. *Journal of Building Physics, 31*(4), 333-360.

Roels, S. and Janssen, H. (2006). A Comparison of the Nordtest and Japanese Test Methods for the Moisture Buffering Performance of Building Materials. *Journal of Building Physics, 30*(2), 137-161.

Samri, D. (2008). Analyse physique et caractérisation hygrothermique des matériaux de construction : approche expérimentale et modélisation numérique. Ph.D. Thesis, Institut National des Sciences Appliquées de Lyon, France

Scheffler, G. A. and Plagge, R. (2010). A whole range hygric material model: Modelling liquid and vapour transport properties in porous media. *International Journal of Heat and Mass Transfer, 53*(1–3), 286-296.

Tariku, F., Kumaran, K. and Fazio, P. (2010a). Integrated analysis of whole building heat, air and moisture transfer. *International Journal of Heat and Mass Transfer, 53*(15–16), 3111-3120.

Tariku, F., Kumaran, K. and Fazio, P. (2010b). Transient model for coupled heat air and moisture transfer through multilayered porous media. *International Journal of Heat and Mass Transfer, 53*(15–16), 3035-0344.

ter Braak, C. J. F. (2006). A Markov Chain Monte Carlo version of the genetic algorithm Differential Evolution: easy Bayesian computing for real parameter spaces. *Statistics and Computing*, 16, 239-249.

van Schijndel, A. W. M. (2009). Integrated modeling of dynamic heat, air and moisture processes in buildings and systems using SimuLink and COMSOL. *Building Simulation, 2*(2), 143-155.

Woloszyn, M. and Rode, C. (2008). Tools for performance simulation of heat, air and moisture conditions of whole buildings. *Building Simulation, 1*(1), 5-24.